



# The Effect of Heat Input on the Mechanical and Corrosion Properties of AISI 304 Electric ARC Weldments

T. E. Abioye<sup>1\*</sup>

<sup>1</sup>Department of Mechanical Engineering, Faculty of Engineering, Federal University of Technology, Akure, PMB 704, Ondo State, Nigeria.

## Author's contribution

*The sole author designed, analyzed and interpreted and prepared the manuscript.*

## Article Information

DOI: 10.9734/BJAST/2017/32846

Editor(s):

(1) Nan Wu, Department of Mechanical and Manufacturing Engineering, University of Manitoba, Winnipeg, Canada.

Reviewers:

(1) Victor A. Adedayo, Institute of Technology, Ilorin, Nigeria.

(2) Siva Prasad Kondapalli, Anil Neerukonda Institute of Technology & Sciences, Visakhapatnam, India.

Complete Peer review History: <http://www.sciencedomain.org/review-history/18924>

**Original Research Article**

**Received 18<sup>th</sup> March 2017**

**Accepted 18<sup>th</sup> April 2017**

**Published 5<sup>th</sup> May 2017**

## ABSTRACT

The mechanical and corrosion performances of austenitic stainless steels arc weld joints in service environments have been established to be influenced by the process parameters used in carrying out the welding process. In this work, the mechanical and corrosion resistance of electric arc weld joints of AISI 304 was investigated at varying process parameters. The welding was carried out using ESAB LHF 400 industrial welding machine. The microstructure of the weld joints was examined using optical microscopy and scanning electron microscopy. The micro-hardness and tensile strength of the welded samples were determined with the aid of Vickers micro-hardness tester and Instron universal testing machine respectively. The electrochemical corrosion of the samples in 3.5% NaCl solution was investigated using potentiostat. The results revealed that good quality arc weld joints are obtainable at a welding current range of 90-130 A and welding speed of 1.7-4.0 mm/s. The microstructure of the weld joints comprises austenite and delta-ferrite phases. The hardness value of the weld joints (ranging within 234-275 HV<sub>0.1</sub>) was found to decrease with increase in the heat energy per unit length of weld. The optimal ultimate tensile stress of 550 MPa was obtained at a heat energy input of 9680 J/mm, whereas the value obtained for the as-received AISI 304 is 560 MPa. The corrosion performance of the arc weld joints is close to that of the as-received AISI 304. However, the corrosion performance of the weld joints decreased with increase in the heat energy input.

\*Corresponding author: E-mail: [teabioye@futa.edu.ng](mailto:teabioye@futa.edu.ng);

*Keywords: Welding; AISI 304; tensile strength; heat input; hardness; corrosion.*

## 1. INTRODUCTION

Austenitic stainless steels have a wide range of applications because of their excellent engineering properties. These properties include high corrosion resistance, good weldability, formability, high impact and tensile strength [1]. They provide high impact strength and corrosion performance at relatively lower cost compared to other alloys such as Inconel 625, Ti-6Al-4V, etc. Like other austenitic stainless steels, AISI 304 has good welding characteristics and is suited to all standard welding methods such as shielded metal arc welding (SMAW), gas tungsten arc welding (GTAW), submerged arc welding (SAW), resistance welding and brazing [2]. Due to its combination of excellent mechanical and corrosion properties, AISI 304 has found applications in a wide variety of corrosive media including foodstuffs, sterilizing solutions and most organic chemicals [3]. Specifically, the material is extensively used in the storing and transportation of liquefied natural gas (whose boiling point is  $-162^{\circ}\text{C}$  under 1 atmosphere) [4]. Also, AISI 304 is widely used as nuclear structural materials for reactor coolant piping and valve bodies [5].

Often, stainless steel parts are joined together using arc welding technique for making sophisticated engineering components and structures. The major issues about arc welding of AISI 304 stainless steel are the large heat affected zone (HAZ) and corrosion damage initiating from the weld joints. According to Karci et al. [6], the heat affected zone refers to that portion of the base metal that has not been melted but the structural or mechanical properties of the metal have been altered by the welding heat. In the past, some work has been done on the arc welding of AISI 304 stainless steel. For example, Oyetunji et al. [7] established that service failure of AISI 304 arc welded joints is due to cracking in the HAZ. Also, performance of the welded structures is usually limited by failure initiation within the HAZ of the base material, particularly within the coarse-grain region of the HAZ adjacent to the weld metal. Therefore, the HAZ is critical to the service performance of welded structures and their reliability under varied loading conditions.

Also, Oyetunji et al. [7] studied the effects of welding speed and power input on the hardness property of AISI 304L heat-affected zone (HAZ) welded with Gas Tungsten Arc Welding (GTAW)

process. The results obtained showed that the hardness property of the HAZ was influenced at varying degrees within the range of welding speeds and power inputs investigated. The influence of heat input on the microstructure and mechanical properties of gas tungsten arc welded 304 stainless steel joints has been a subject of investigation by Kumar and Shahi [4]. Three heat input combinations designated as low heat (2.563 kJ/mm), medium heat (2.784 kJ/mm) and high heat (3.017 kJ/mm) inputs were selected from the operating window of the gas tungsten arc welding process (GTAW). The results of this investigation indicated that the joints made using low heat input exhibited higher ultimate tensile strength (UTS) than those welded with medium and high heat input. Significant grain coarsening was observed in the heat affected zone (HAZ) of all the joints and it was found that the extent of grain coarsening in the heat affected zone increased with increase in the heat input. The microstructure and mechanical properties of an austenitic steel weldments have been investigated by Chennaiah et al. [8]. It was found that the formation of austenite phase is believed to be beneficial to the corrosion and mechanical performance of the weldment whereas the delta ferrite phase is undesirable because it is a softer phase and makes the weldments susceptible to corrosion damage. Prasad et al. [9] conducted a study on the weld quality characteristics of pulsed current micro-plasma arc welding of SS 304L sheet. It was established that a high quality weld joints can be obtained through optimal combination of the welding parameters.

Choubey and Jatti [1] researched on the effect of heat input on tensile strength, micro-hardness and microstructure of austenitic 202 grade stainless steel weldments produced by shielded metal arc welding (SMAW). It was found that the tensile strength decreases with increase in heat input. The effects of the varying welding parameters on the mechanical properties of low carbon steel has been a subject of investigation by Bodude and Momohjimoh [10]. One of the findings is that the cooling rate which is a function of the heat input utilised determines the proportion of ferrite and pearlite formation in the microstructure of the weldments. This, in turn, influences the tensile, impact and hardness behaviors of the weldments. Liang et al. [11] studied the corrosion resistance of welds in type 304L stainless steel made with nickel-copper-

ruthenium welding consumable. The results obtained showed that the welded joints exhibited good corrosion properties which were better than the weldments made using nickel-copper-palladium consumable which is commonly used.

Though some work has been reported on the effect of variation of heat input on the hardness and mechanical properties of AISI 304 stainless steel arc welded joints, the effect of heat inputs on the corrosion properties of the welded joints has not been well researched. Also, the individual effect of the welding parameters and the relative significance of each of the process parameters on the mechanical and corrosion performance of the electric arc weldments has not been reported. The aim of the research is to investigate the effects of welding parameters and heat energy input on the mechanical and corrosion performance of the arc weld joints produced within a process window.

## 2. MATERIALS AND METHODS

### 2.1 Materials

Austenitic stainless steel AISI 304 was purchased from The Metal Centre, Wednesbury, Great Britain and is the base material to be used for the research. The chemical composition of

the AISI 304 as received from the supplier is given in Table 1. The base material was cut into plates of dimension 100 mm X 50 mm X 8 mm using power hacksaw. Twenty four (24) of such samples were made. It is noteworthy to state that prior to the welding process, the plates were cleaned and degreased in order to remove different forms of contaminants.

The welding electrode used for the production of the weldment is of specification “AWS 308L -16”. Based on the British Standards, gauge 12 electrodes with nominal diameter of 2.5 mm were used for the arc welding of the stainless steel. This was preferred in order to have an electrode that is suitable for the range of the welding current to be used.

### 2.2 Welding Process

Fig. 1 shows the electric arc welding process. The arc welding process was performed at the Mechanical Engineering Workshop, Federal University of Technology, Akure (FUTA) using ESAB LHF 400 offshore industrial welding machine. All standard welding procedures was adhered to. After some trial experiments were done, the arc welding was carried within the range of parameters (process window) defined in the Table 2.

**Table 1. Elemental composition of the as-received AISI 304 stainless steel**

Element	Fe	C	Si	Mn	P	Cr	Ni	N
Composition (wt.%)	71.56	0.021	0.43	1.52	0.03	18.3	8.1	0.04

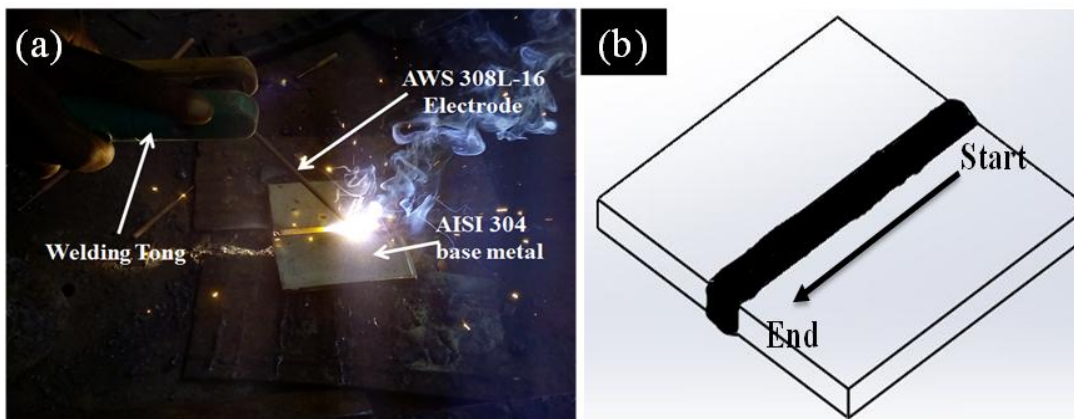


**Fig. 1. (a) A picture showing the electric arc welding of the AISI 304 plates and (b) a schematic describing the welding direction**

**Table 2. The range of parameters used for the arc welding process**

Parameter	Symbol	Value	Unit
Welding current	I	90 - 130	A
Welding voltage	V	220	V
Welding Speed	S	1.7 - 4.0	mm/s
Root gap		2.5	mm

The current and speed of welding were varied while the voltage was kept constant at 220 V. Prior to each welding process, a root gap of 2.5 mm was allowed between the metal plates to be joined together so as ensure high quality weld with deep penetration. The welding speed (S) and heat input per unit length of weld (H) for each combination of the parameters were calculated using equations 1 and 2 respectively. H is the heat input per unit length of weld (J/mm), L is the length of weld (mm) which was kept constant at 100 mm while T denotes the time taken to weld 100 mm length (s).

$$S = \frac{L}{T} \quad (1)$$

$$H = \frac{VI}{S} \quad (2)$$

Each AISI 304 weldment was made in three passes. As shown in Fig.1b, each pass commenced from the same side of the plate identified as the welding start point (Start) and a cooling time of 60 seconds was allowed in-between the successive passes. Weldments were produced at different welding parameters giving nine (9) welding conditions, as presented in Table 3. Three different weldments were done at each welding condition so as ensure the validity and reliability of the results obtained.

**Table 3. Heat energy per unit length of weld obtained at varying speed and current**

I (A)	V (V)	S(mm/s)	H (J/mm)
90	220	4	4950
90	220	2.5	7920
90	220	1.7	11647
110	220	4	6050
110	220	2.5	9680
110	220	1.7	14235
130	220	4	7150
130	220	2.5	11440
130	220	1.7	117160

### 2.3 Microstructural Characterisation

Samples of dimension 40 mm × 10mm × 8mm were cut from the weldments. All samples were

cut in the middle of the weld because it is believed that it takes few seconds for welding process to be stable. All weld samples were ground and polished to 1µm surface finish. Samples formed at high, medium and low heat input were selected and examined for microstructural changes using optical microscopy and a combination of scanning electron microscopy (SEM) and energy dispersive X-ray spectroscopy (EDXS). Prior the microstructural examination, the polished samples were etched in 10 g of oxalic acid saturated in 100 ml distilled water for a period of 30 minutes.

### 2.4 Hardness Test

Micro-hardness test was carried out on all the weldment samples formed using Vickers hardness tester. Ten indentations were randomly made, along the centerline of the joint, on each of the test samples. A gap of about 3 mm was allowed in-between the indentations. The indentations were made using a 100 g load and a dwell time of 10s.

### 2.5 Tensile Test

Three tensile test samples per each heat input were prepared using British E08 standard. A schematic of the tensile test sample according to the standard is shown in Fig. 2. Samples were cut across the weld joints. The test was carried out using Instron Universal Testing Machine at Engineering. The test was done using an extension rate of 2 mm/min. Each test is completed after fracture occurred.

### 2.6 Corrosion Test

Electrochemical corrosion testing was performed on the as-received AISI 304 and three selected weld samples obtained at low, medium and high heat input values. These tests were carried out for all the samples according to the guidelines stated in ASTM standards G5-94 and G61-86 respectively. The samples were cut into 1 cm x 1 cm to give it an exposed area of 1 cm<sup>2</sup>. Thereafter, samples were ground to the same thickness so as to reduce variations in the

microstructures of the samples' top surfaces. The samples were later hot mounted on non-conductive resin and later drilled so as to make an electrical contact with the sample. Each sample was carefully prepared so as to make sure that only the  $1\text{cm}^2$  (i.e.  $100\text{mm}^2$ ) surface of the sample is exposed to the electrolyte.

In each test, the sample (i.e. the working electrode) was immersed in the electrolyte (de-aerated 3.5 wt.% NaCl solution) and was allowed to stabilise for 60 minutes before polarizing the potential against the reference electrode (Ag/AgCl). A platinum plate was used as the counter electrode. A potentiostat was used for the test. The electrode potentials were measured with a scan rate of  $1\text{mV/s}$  and potential range of  $-0.25 - 1.25\text{mV}$ . The corrosion test was conducted in a salty environment so as to represent the intended application environment.

### 3. RESULTS AND DISCUSSION

#### 3.1 Welding Quality

The suitable welding current for the plate samples was firstly established to be within the range of  $90 - 130\text{A}$ . All weld joints obtained at current values below  $90\text{A}$  were poorly formed due to insufficient or incomplete weld penetration. This indicates that for the range of speed utilized in this work, the heat energy per unit length of weld obtained at current values below  $90\text{A}$  is insufficient to give full weld penetration hence, high quality weld. Also, at current value above  $130\text{A}$ , the heat energy is excessive as the melting instead of welding of the plates was observed. Fig. 3 presents the pictures of some quality weld obtained within the chosen process window.

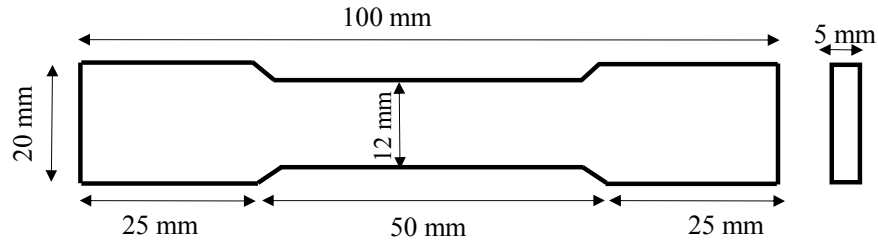


Fig. 2. A schematic of the tensile test sample

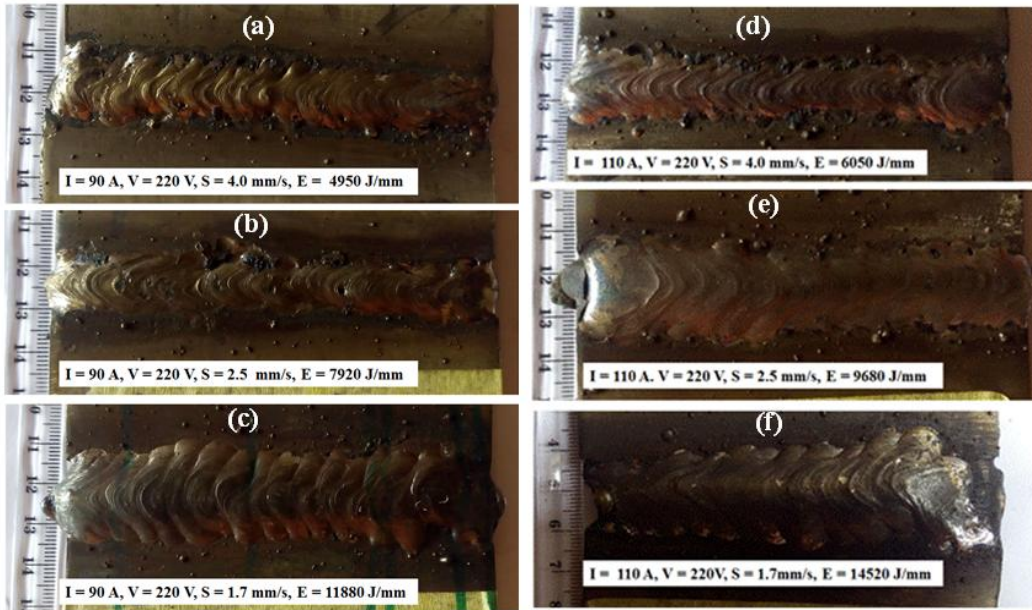


Fig. 3. Pictures of the electric arc weldments of AISI 304 obtained within the process window



### 3.2 Effects of the Welding Parameters on the Bead Width

Fig. 4 reveals the influence of the welding speed and current on the width of the weld beads. The bead width was measured and it was discovered that the width of the bead decreases with increasing welding speed. This can be explained by the fact that the electrode interacted longer with a unit length of the base metal at lower

speed. As a result, more heat energy is available for welding per unit length of the base metal therefore, resulting in wider bead. Conversely, at higher speed, the energy per unit length of weld is smaller hence, a smaller bead was generated. Similarly, it was observed that the bead width increases with increasing current. This is due to the fact that heat energy dissipated per unit length of the weld is proportional to the welding current, as evidenced in equation 2.

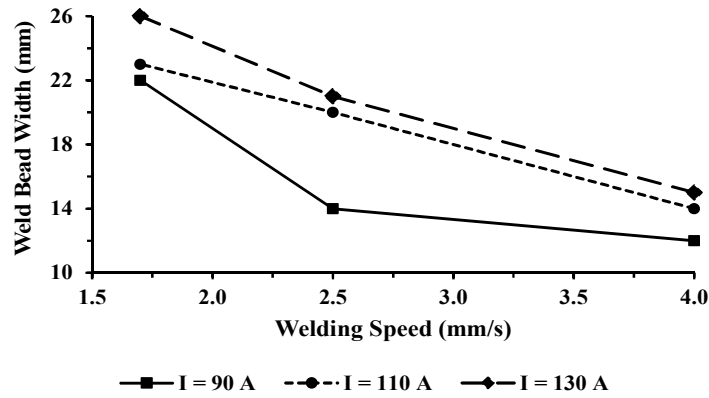


Fig. 4. The variation of the weld bead width with the speed and current

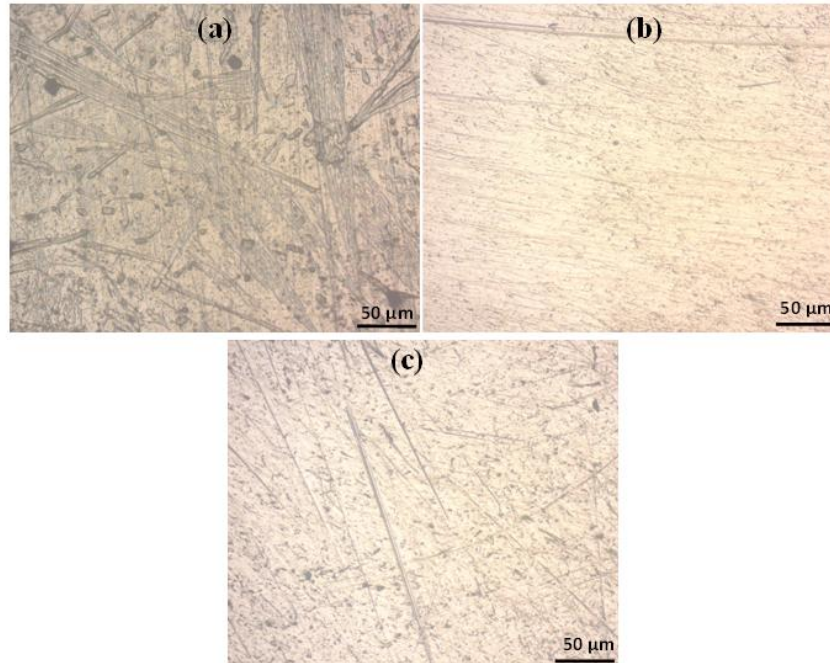


Fig. 5. Optical images of the weld region of the AISI 304 arc weldments. (a) I = 90 A, V = 220 V, S = 1.7 mm/s, H = 11880 J/mm (b) I = 110 A, V=220V, S = 1.7 mm/s, H = 14520 J/mm, (c) I= 130 A, V=220V, S = 1.7 mm/s, H = 17160 J/mm

### 3.3 Microstructure of the Weldments

The optical micrographs of the fusion zone of the three weld samples made at 11880 J/mm (low), 14520 J/mm (medium) and 17160 J/mm (high) heat energy per unit weld length are presented in Fig. 5. It was observed that weld joints were void cracks and visible pores. This is evidence that all weldments made within the process window were of good quality.

The SEM (Back Scattered Electron) images of the weld zone for the three selected samples are presented in Fig. 6. The images reveal two prominent phases which are (1) a randomly dispersed black nodules and (2) a continuous grey-like phase. Similar observation has been

reported in the past by Chennaiah et al. [8]. The black nodules and continuous grey-like phase were identified as delta ( $\delta$ ) ferrite and austenitic phase respectively.

As seen in the Fig.6, the  $\delta$  ferrite phase (black nodules) appears to be of lower number density in the weld sample obtained at low heat input (11880 J/mm) when compared with the weld sample formed at 17160 J/mm. According Chennaiah et al. [8] and Bodude and Momohjimoh [10] the formation of austenite is believed to be beneficial to the corrosion and mechanical performance of the weldment. However, the delta ferrite has been proved to be a softer phase and is undesirable in the weld.

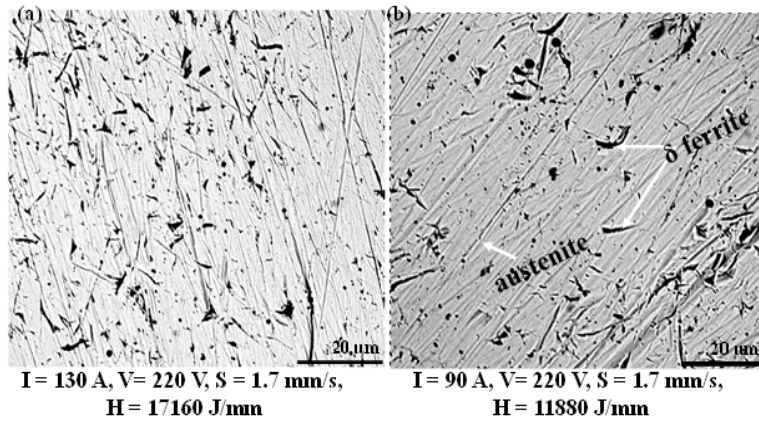


Fig. 6. Back scattered electron (SEM) micrographs showing the weld zone of the AISI 304 arc weldments at low and high heat input

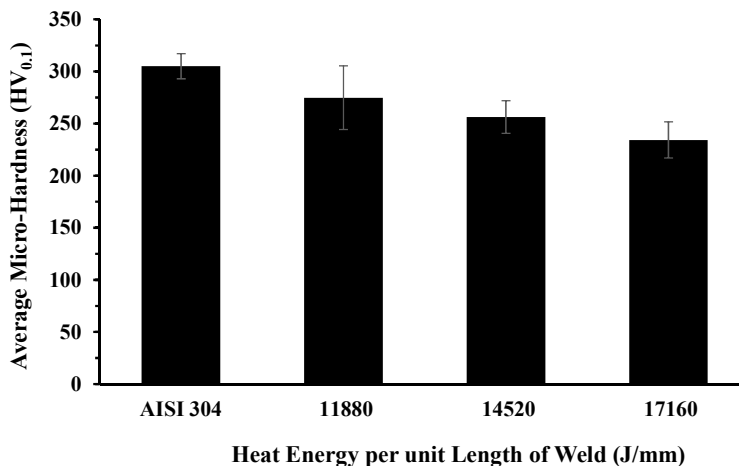


Fig. 7. The variation of the micro-hardness of the weld joints with the heat energy input per unit length of weld

### 3.4 Micro-hardness

The results of the Vickers micro-hardness on the three selected samples and the as received AISI 304 plate are presented in Fig. 7. Each value presented is an average of 10 indentations made at different locations along the weld zone of the weldments. The micro-hardness values obtained at 11880 J/mm, 14520 J/mm and 17160 J/mm are  $275 \pm 31$ ,  $256 \pm 16$ ,  $234 \pm 17$  HV<sub>0.1</sub> respectively. All the values are lower than the value obtained for the as-received AISI 304 ( $305 \pm 12$ ). Also, the hardness values decreased with increasing the heat energy per unit weld length.

The observed smaller value of the hardness performance of the tested hardness samples relative to the as-received AISI 304 can be attributed to the relative finer grain size of the microstructure observed in the as-received plate compared with the weld joints. The cooling at the weld joints is slower therefore resulting in coarse structure. Also, the formation of the  $\delta$  ferrite phases after solidification partially contributed to the weaker surface observed in the weld joints. The decreasing hardness with the increasing heat energy per unit length of weld is due to increased heat energy dissipation and slower cooling rate or solidification of the molten metal at the weld zone. The result is in agreement with the past findings of Oyetunji et al. [7]. The increasing  $\delta$  ferrite content with increasing heat energy per unit weld length would have contributed to the decreased hardness observed at higher heat energy input.

### 3.5 Tensile Strength

Fig. 8 shows the variation of the tensile strength of the weld samples with the heat energy per unit weld length. First, the ultimate tensile strength (UTS) increases with the heat input per unit weld length until an optimal point ( $549.6 \pm 13$  MPa) was reached after which the UTS was decreasing with further increase in the heat energy input. The optimal point is obtained at a heat input of 9680 J/mm with the welding parameters of 110 A and 2.5 mm/s speed.

The first increase in the UTS can be attributed to a progressive increase in the weld penetration due to increasing heat input. It is believed that after full penetration was obtained further increase in the heat energy input per unit length of weld resulted in decrease in the UTS due to the increased grain size and higher volume fraction of the softer phase (i.e.  $\delta$  ferrite) in the

microstructure of the weld joints. The decreasing trend of UTS with the increasing heat energy input is in agreement with the findings of Choubey and Jatti [1]. The UTS of the as-received AISI 304 stainless steel was found to be  $560.2 \pm 11$  MPa which is slightly higher than the optimal value obtained for the weld joints.

### 3.6 Corrosion Performance

The cyclic polarization curve for as-received AISI 304 and the three selected weld samples obtained at low, medium and high heat energy per unit weld length are presented in the Fig. 9. The result revealed that the corrosion performances of the weldments are close to that of the as-received AISI 304. The as-received AISI 304 has the highest corrosion potential (-0.48 mV) whereas the corrosion potential for the arc weldments obtained at 11880 J/mm, 14520 J/mm and 17160 J/mm are -0.54, -0.52 and -0.62 mV respectively.

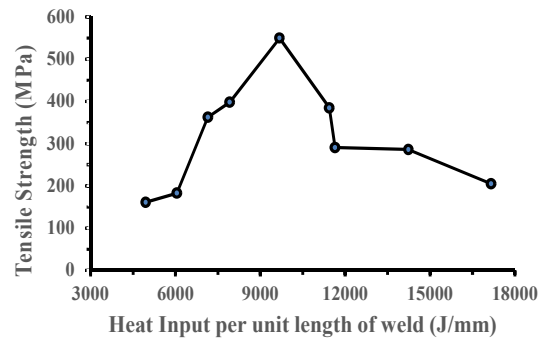


Fig. 8. The variation of the tensile strength of the weldments with respect to the heat input per unit length of weld

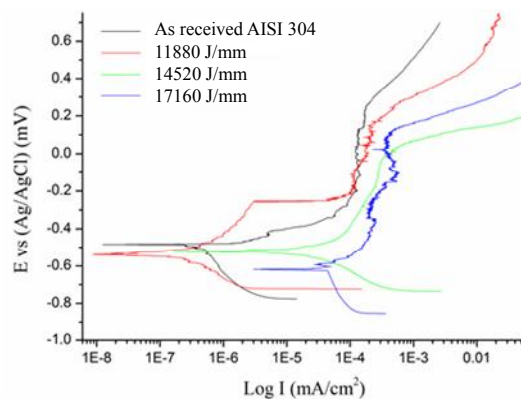


Fig. 9. Cyclic polarisation curve of as-received AISI 304 and electric arc AISI 304 weldments at varying heat energy input



Also, the as-received AISI 304 has the lowest current density of  $1.03 \times 10^{-4}$  mA/cm<sup>2</sup>. The value of the current density of weld samples increases as the heat energy input increases. This shows that the as-received AISI 304 performed best whereas the corrosion performance of the weldments decreases as the heat energy input increases. The reason can be traced to the increasing amount of  $\delta$ -ferrite in the weld samples as the heat energy input increased. The presence of  $\delta$ -ferrite in the weld metals has been established to be detrimental to their corrosion performance.

#### 4. CONCLUSION

The effects of heat energy input on the mechanical and corrosion properties of the electric arc AISI 304 weld joints have been successfully investigated in this study. High quality weld joints that are free of visible pores and cracks were produced within the process window utilised in this work. The weld bead width varied directly with the welding current and indirectly with the welding speed. The microstructure of the weld joints consists of austenite and traces of  $\delta$ -ferrite phases. The number density of the  $\delta$ -ferrite in the weld joint microstructure increased with the heat energy per unit weld length. The heat input affects the weld joint hardness (ranging between 234 – 275 HV<sub>0.1</sub>) negatively. Full weld penetration was found to be key to obtaining high tensile strength of the weld joint. The tensile strength of the weld joint, after full penetration is achieved, decreased (from 550 -260 MPa) with increasing the heat input. The corrosion performance of the weld joints is close to the as-received AISI 304 however, the performance decreased with the increase in the heat energy input.

#### ACKNOWLEDGEMENT

The author wish to appreciate the technical assistance of Engr Charles Odanaogun and Mr Daisi of Mechanical Engineering Department, Federal University of Technology, Akure, Nigeria towards the success of this research.

#### COMPETING INTERESTS

Author has declared that no competing interests exist.

#### REFERENCES

1. Choubey A, Jatti VS. Influence of heat input on the mechanical properties and

- microstructure of austenitic 202 grade stainless steel weldments. WSEAS Journal. 2014;9:222-228.
2. Kotecki D, Armao F. Stainless steel properties- where to weld them, how to use them. Stainless Steels Welding Guide. Lincoln Electric Company; 2003.
  3. Tabish TA, Abbas T, Farhan M, Atiq S, Butt TZ. Effect of heat input on microstructure and mechanical properties of the TIG welded joints of AISI 304 stainless steel. International Journal of Scientific & Engineering Research. 2014;5(7):2-3.
  4. Kumar S, Shahi AS. Effect of heat input on the microstructure and mechanical properties of gas tungsten arc welded AISI 304 stainless steel joints. Journal of Materials and Design. 2011;32.
  5. Yan J, Gao M, Zeng X. Study on the microstructure and mechanical properties of 304 stainless steel joints by TIG, Laser and Laser-TIG hybrid welding. Journal of Optics and Lasers in Engineering. 2010;48:512-517.
  6. Karci F, Kacar R, Gunduz S. The effect of process parameter on the properties of spot welded cold deformed AISI 304 grade austenitic stainless steel. Journal of Materials Processing Technology. 2008;209: 4011-4019.
  7. Oyetunji A, Kutelu BJ, Akinola AO. Effects of welding speeds and power inputs on the hardness property of type 304L austenitic stainless steel heat-affected zone. Journal of Metallurgical Engineering. 2013;2(4):124-129.
  8. Chennaiah MB, Kumar PN, Rao KP. Effect of heat input and heat treatment on the mechanical properties of Is2062 Is103 Cr 1 steel weldments. International Journal of Advances in Materials Science and Engineering. 2015;4(3):17-24.
  9. Prasad KS, Rao CS, Rao DN. A study on weld quality characteristics of pulsed current micro plasma arc welding of SS304L sheet. International Transaction Journal of Engineering, Management, & Applied Sciences & Technologies. 2011;2(4):437-446.
  10. Bodude MA, Momohjimoh I. Studies on effects of welding parameters on the mechanical properties of welded low-carbon steel. Journal of Minerals and

- Materials Characterization and Engineering. 2015;3: 142-153.
11. Liang D, Sowards JW, Frankel GS, Alexandrov BT, Lippold JC. Corrosion resistance of welds in type 304l stainless steel made with a Nickel-Copper-Ruthenium welding consumable. Journal of Corrosion Science. 2010;52:2439-2451.

---

© 2017 Abioye; This is an Open Access article distributed under the terms of the Creative Commons Attribution License (<http://creativecommons.org/licenses/by/4.0>), which permits unrestricted use, distribution, and reproduction in any medium, provided the original work is properly cited.

*Peer-review history:*  
*The peer review history for this paper can be accessed here:*  
<http://sciencedomain.org/review-history/18924>